Computers and Geotechnics 72 (2016) 28–41

Contents lists available at ScienceDirect

Computers and Geotechnics

journal homepage: www.elsevier.com/locate/compgeo

Research Paper

# Effect of particle shape and validity of $G_{max}$ models for sand: A critical review and a new expression

Meghdad Payan, Arman Khoshghalb, Kostas Senetakis, Nasser Khalili *

*School of Civil and Environmental Engineering, UNSW Australia, Sydney 2052, Australia*

ARTICLE INFO

*Article history:*
Received 18 August 2015
Received in revised form 3 November 2015
Accepted 3 November 2015

*Keywords:*
Dynamic shear modulus
Sand
Resonant column
State parameter
Particle shape

ABSTRACT

Shear modulus of soils at small strains, $G_{max}$, is an important parameter in the design of geo-structures subjected to static and dynamic loading. Numerous models have been proposed in the literature for the prediction of $G_{max}$ for saturated and dry sands. In this work, a novel approach is proposed, based on the concept of state parameter, for the examination of the validity of $G_{max}$ equations in capturing the effects of void ratio and confining pressure on the small-strain behavior of granular soils. Four expressions of $G_{max}$ from the literature are examined. It is shown that while the expressions examined may predict the measured values of $G_{max}$ with some level of accuracy, dependencies to the state parameter are observed when the results are plotted against the state parameter. This is attributed to the exclusion of the effect of particle shape in the determination of the model parameters. To alleviate this deficiency, a new expression of $G_{max}$ for dry and saturated sands is proposed and validated using a comprehensive set of resonant column test data performed at a range of initial void ratios, confining pressures, particle shapes and grain size distributions.



## 1. Introduction

Shear modulus plays a fundamental role in the analysis and design of geotechnical structures subjected to static and dynamic loading. Of particular interest is the modulus at very small strains (less than $10^{-3}$%), where pure elasticity is assumed to govern the soil behavior. Precise determination of small-strain shear modulus of soils (typically denoted by $G_{max}$) has been the focus of many investigations in the past. These have included in-situ geophysical approaches, such as up-hole, down-hole and cross-hole techniques [1], and laboratory experiments using resonant column and bender element apparatus [2–5].

The first comprehensive studies of small-strain shear modulus of soils date back to 1960s and early 1970s [2,6–10], which also coincided with the first attempts to develop the resonant column apparatus [2]. Focusing on the behavior of dry and saturated sands, these investigations showed that shear modulus at small strains depended primarily on the void ratio of the soil, $e$, and the mean effective confining pressure, $p'$. Similar observations were also made by Hardin and Black [7,8], Hardin and Drnevich [11], Hardin [3], Iwasaki et al. [4], Kokusho [12], Chung et al. [13], Yu and Richart [14], Saxena and Reddy [15], and Jamiolkowski et al. [16]. These studies have led to the development of a general expression for the estimation of the small-strain shear modulus of sands in the form of:

$$G_{max} = A \times f(e) \times \left(\frac{p'}{p_a}\right)^n \quad (1)$$

in which, $p_a$ is the reference atmospheric pressure, $f(e)$ is the void ratio function, and $A$ and $n$ are the model parameters to be determined experimentally. Various void ratio functions, $f(e)$, are presented in the literature, typically in the form of ratio or power relationships, inspired by the seminal contributions of Hardin and Richart [2] and Jamiolkowski et al. [16]. Parameters $A$ and $n$, are in turn linked to the grain size distribution of the soil through the coefficient of uniformity, $C_u$, and the mean grain size, $d_{50}$ [17–23]. Cho et al. [24] were first to point out the strong dependency of $A$ and $n$ on the shape of the soil particles, although they overlooked the effect of grain size distribution and soil density in their investigation. The effect of particle shape was also recognized in the early studies of Hardin and Richart [2] through the introduction of two models of $G_{max}$: one for sands of relatively regular shape, such as natural river sand, and the other for sands with irregularly shaped grains, such as crushed rock. Similarly, Senetakis et al. [22] developed $G_{max}$ models in two categories depending on the shape of the particles in the sand. Nevertheless, there currently exist no expressions of $G_{max}$ that take into account the effect of particle shape in a systematic manner. Indeed, as will be shown in this

* Corresponding author.

http://dx.doi.org/10.1016/j.compgeo.2015.11.003
0266-352X/

work, ignoring the effect of particle shape can lead to incorrect representation of influences of void ratio, confining pressure and soil stress state, leading to expressions of $G_{max}$ with relatively limited practical applicability.

Two distinct contributions are made in this work. Firstly, an entirely new approach is proposed, based on the concept of *state* parameter, for evaluating the validity of $G_{max}$ expressions in capturing the influences of void ratio and confining pressure on the small-strain behavior of granular soils. Four expressions of $G_{max}$ from the literature are examined and it is shown that while they may predict the measured values of $G_{max}$, i.e. for a specific type of soil, significant scatter occurs when the results are plotted against the *state* parameter. This is attributed to the misrepresentation of the soil stress *state* due to the exclusion of the effect of particle shape in the determination of the model parameters. Secondly, a new expression for $G_{max}$ is proposed for sands in order to capture the soil stress state and the combined effects of particle shape, grain size distribution, void ratio and mean effective confining pressure in a consistent manner. The applicability and validity of the new expression are demonstrated using experimental data for a range of initial void ratios, mean effective confining pressures and particle shapes.

## 2. State parameter

Thermodynamically, a set of parameters defining the state of a system are referred to as the state variables or state parameters. Some of the physical entities used for this purpose in geotechnical engineering include: void ratio, confining pressure, stress ratio, pre-consolidation pressure, overconsolidation ratio (OCR), relative density, etc. Once the state parameters for a system are identified, then the response of the system to perturbations in the state

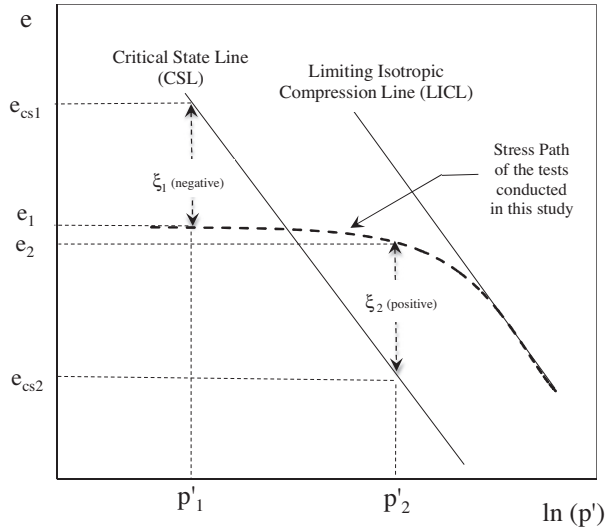


**Fig. 1.** State parameter concept.

parameters can be quantified by invoking a suitably configured constitutive model in terms of the state parameters.

Following the framework of the critical state soil mechanics, void ratio and mean effective confining pressure may be selected as the suitable parameters defining the state of a saturated or dry sand subjected to isotropic loading only [5]. In other words, in such a system, the influence of the stress history, at any confining pressure, may solely be expressed through the use of the void ratio. This is reflected in the general Eq. (1) and other equations proposed in the literature that use $e$ and $p'$ as the state variables for qualification of small-strain shear modulus of sands [15,18,21,22]. If an expression correctly accounts for the state of a sample on the variation of $G_{max}$ with $e$ and $p'$, then other state variables will be redundant and must have no influence in the estimation of $G_{max}$. This is exploited in this work to independently verify the appropriateness of expressions proposed in the literature for the prediction of $G_{max}$ for sands, in particular in relation to capturing the effects of $e$ and $p'$.

For fine-grained soils, overconsolidation ratio (OCR) is an appropriate state variable for the independent verification of $G_{max}$ equations [5]. However, for granular materials, high confining pressures are required to reach limiting isotropic compression line (LICL) which renders it difficult to use OCR for the verification purposes. For such soils, the concept of the *state* parameter is more appropriate and is adopted in this study to verify the small-strain shear modulus expressions for sandy soils.

*State* parameter, $\xi$, was first introduced by Been and Jefferies [25] and Been et al. [26], and is the difference between the current void ratio, $e$, or specific volume, $v = 1 + e$, of the soil and the void ratio or specific volume at the critical state for a given confining pressure. Based on the state of the soil in the $e - \ln p'$ plane, the state parameter can simply be obtained by measuring the vertical distance of the stress point with respect to the critical state line (CSL), as shown in Fig. 1. As such it can attain positive or negative values based on the relative state of the soil with respect to the critical state line (CSL). In this study, the critical state soil mechanics concepts for sand [27–30] are introduced for the examination of $G_{max}$ expressions through the state parameter.

## 3. Validity of expressions for $G_{max}$

Numerous empirical equations have been proposed in the literature for the prediction of the small-strain shear modulus of dry

**Table 2**
Basic properties of sands tested by Jovicic and Coop [31].

| Sand | Grading | | | | Critical state line parameters | |
|---|---|---|---|---|---|---|
| | $d_{50}$ | $C_u$[a] | $C_c$[a] | USCS | $\lambda$[b] | $\Gamma$[b] |
| Ham River Sand | 0.30 | 1.50 | 1.04 | SP | 0.16 | 2.96 |
| Decomposed Granite | 1.50 | 12.70 | 1.72 | SW | 0.09 | 2.04 |

[a] $C_u = d_{60}/d_{10}$; $C_c = (d_{30})^2/(d_{10} \cdot d_{60})$.
[b] $\lambda$: Slope of critical state line; $\Gamma$: intercept of critical state line.

**Table 1**
Four expressions for the prediction of small-strain shear modulus of sands.

| Model | General form | $A$ | $x$ | $n$ |
|---|---|---|---|---|
| Menq [18] | $A \cdot e^x \cdot (p'/p_a)^n$ | $67.1\,C_u^{-0.2}$ | $-1 - \left(\frac{d_{50}(\text{mm})}{20}\right)^{0.75}$ | $0.48\,C_u^{0.09}$ |
| Saxena and Reddy [15] | $A \cdot \frac{1}{0.3+0.7e^2} \cdot p_a^{1-n} \cdot p'^n$ | 428.2 | – | 0.574 |
| Wichtmann and Triantafyllidis [21] | $A \cdot \frac{(x-e)^2}{1+e} \cdot p_a^{1-n} \cdot p'^n$ | $1563 + 3.13\,C_u^{2.98}$ | $1.94\exp(-0.066\,C_u)$ | $0.40\,C_u^{0.18}$ |
| Senetakis et al. [22] | $A \cdot e^x \cdot (p'/p_a)^n$ | $57.01 - 5.88\,C_u$ | $-0.28\,C_u - 0.98$ | 0.47 |

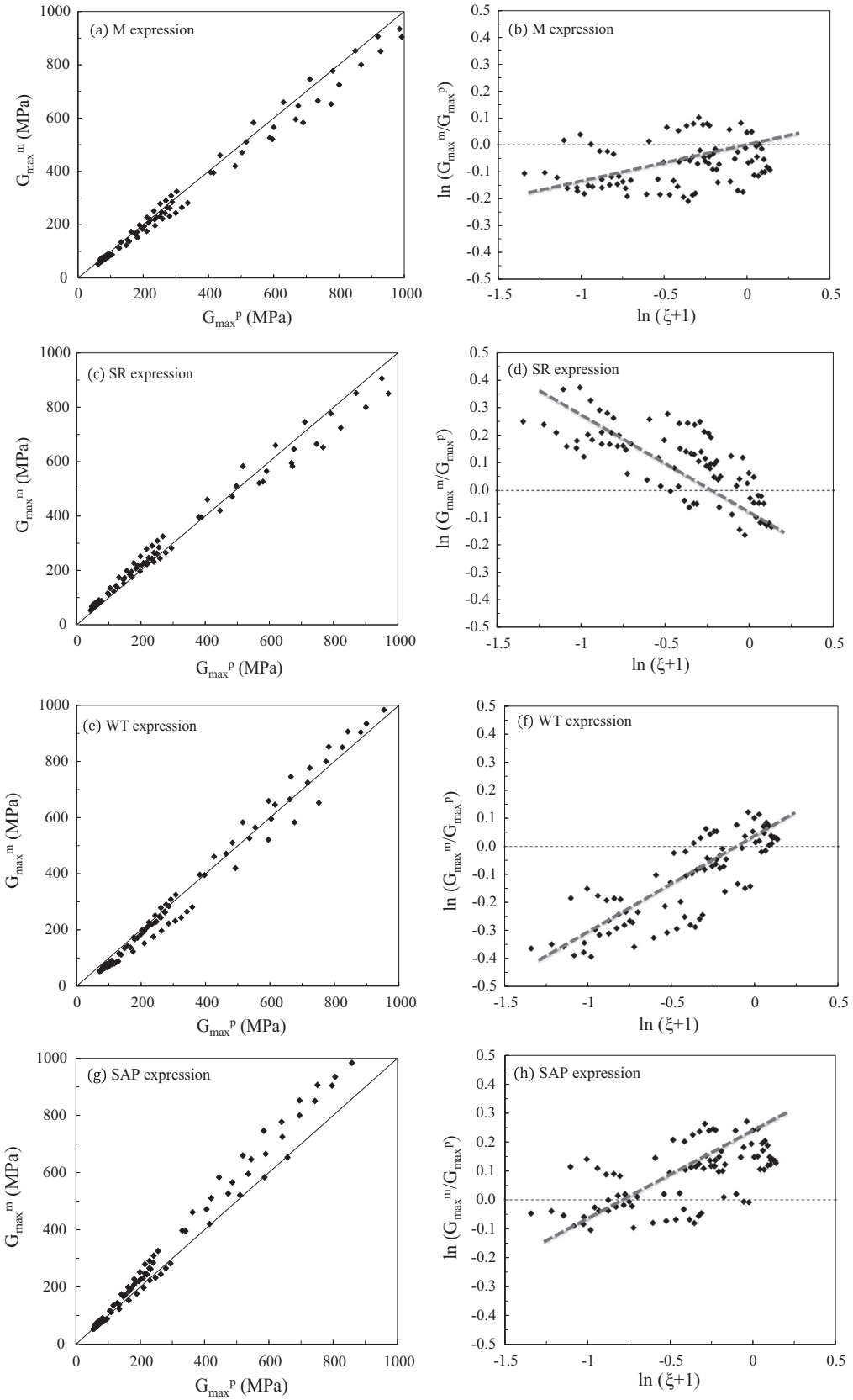


**Fig. 2.** State parameter test results for Ham River sand, Measured against predicted $G_{max}$ values and the influence of the state parameter on different $G_{max}$ models (experimental results by Jovicic and Coop [31]).

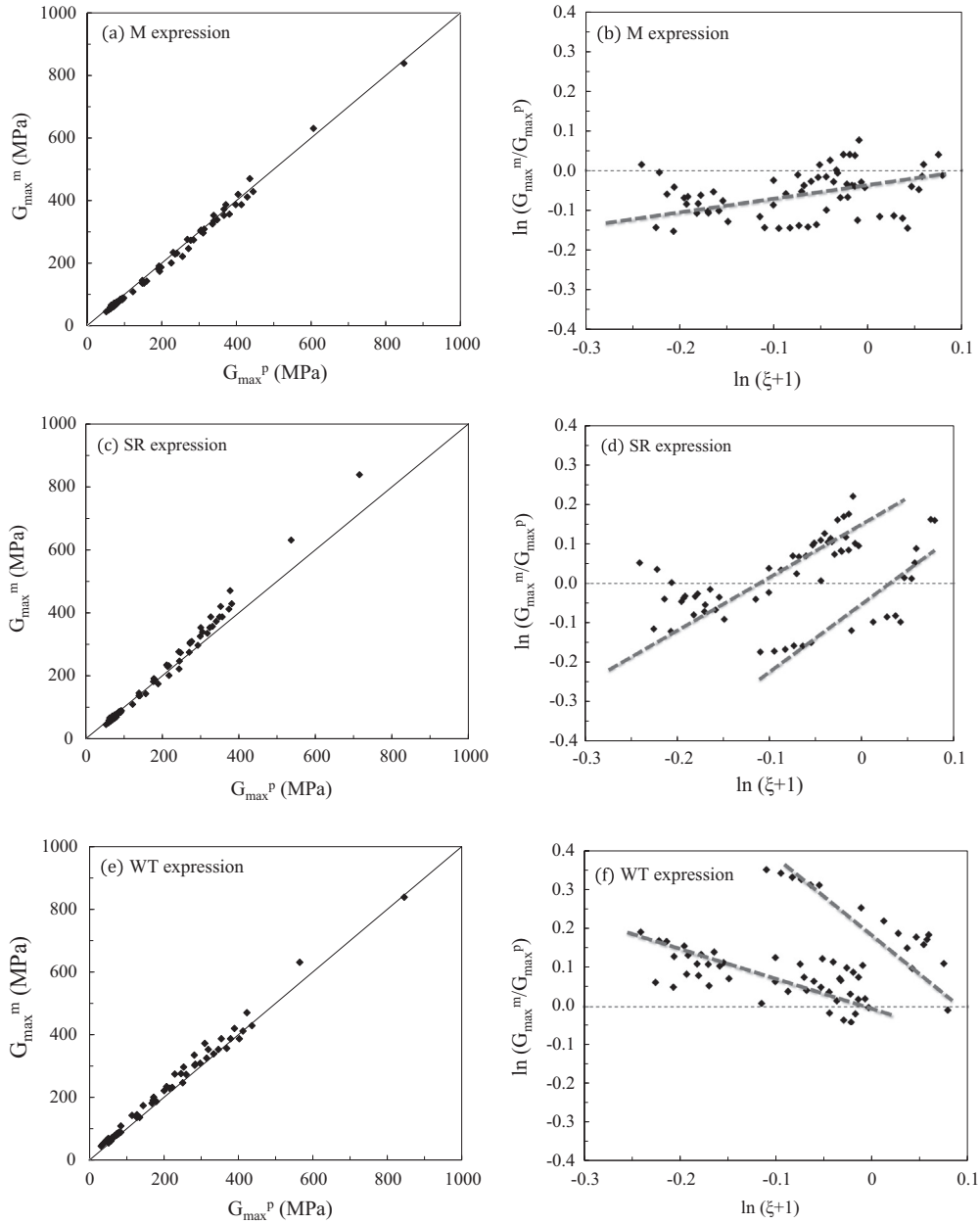


**Fig. 3.** State parameter test results for decomposed granite sand, measured against predicted $G_{max}$ values and the influence of the state parameter on different $G_{max}$ models (experimental results by Jovicic and Coop [31]).

**Table 3**
Tested soil properties for resonant column experiments.

| Test sand | Laboratory material | Grain size distribution | | |
|---|---|---|---|---|
| | | $d_{50}$ | $C_u$ | $C_c$ |
| W | White (Blue circle) Sand | 0.24 | 1.69 | 0.90 |
| N | Newcastle Sand | 0.33 | 1.94 | 1.25 |
| US | Uniform Sydney Sand | 0.36 | 1.18 | 0.96 |
| BL1 | Blue Sand 1 | 1.66 | 1.41 | 0.94 |
| BL2 | Blue Sand 2 | 1.94 | 2.80 | 0.97 |
| BL3 | Blue Sand 3 | 1.88 | 4.11 | 1.22 |
| BL4 | Blue Sand 4 | 1.01 | 8.22 | 1.06 |
| 50UB-50UBL | 50% Uniform Bricky, 50% Uniform Blue Sand | 0.54 | 1.96 | 1.01 |
| 70UB-30UBL | 70% Uniform Bricky, 30% Uniform Blue Sand | 0.49 | 2.01 | 1.10 |
| 30UB-70UBL | 30% Uniform Bricky, 70% Uniform Blue Sand | 0.59 | 1.99 | 1.10 |

and saturated sands. To demonstrate how the *state* parameter can be used for the validation of $G_{max}$ formulas, expressions proposed by Saxena and Reddy [15], Menq [18], Wichtmann and Triantafyllidis [21], and Senetakis et al. [22], denoted here by SR, M, WT and SAP models, respectively, are examined in this study. The essential features of the four expressions are summarized in Table 1. The data used in the validation work was due to Jovicic and Coop [31], obtained using bender element tests on samples of Ham river sand and decomposed granite. The properties of the two test soils, including the critical state parameters, are summarized in Table 2.

The results of the validation work using the Ham River sand data is presented in Fig. 2. For each expression, two separate plots are presented: one in terms of the measured small-strain shear modulus ($G^m_{max}$) versus the predicted small-strain shear modulus ($G^p_{max}$) and the other in terms of $\ln(G^m_{max}/G^p_{max})$ versus $\ln(1+\xi)$, in which $\xi$ is the state parameter. As can be observed from the

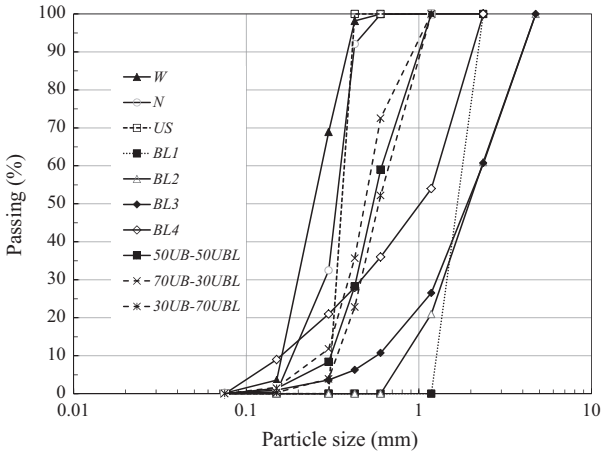


**Fig. 4.** Particle size distribution curves for tested materials.

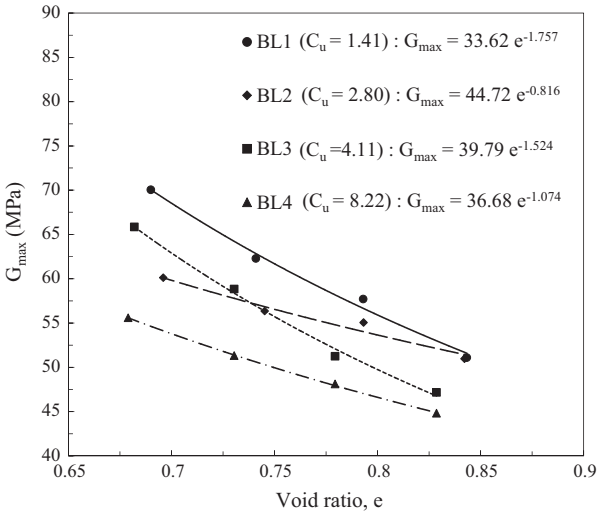


**Fig. 5.** Variation of small-strain shear modulus ($G_{max}$) with void ratio ($e$) for Blue sands with different coefficients of uniformity under 100 kPa isotropic confining pressure.

variation of $\ln(G^m_{max}/G^p_{max})$ versus $\ln(1+\xi)$, there is a clear trend (shown by the dashed lines) and dependency to the *state* parameter in these formulas. This implies that in these expressions the effect of void ratio and mean effective confining pressure, and hence the soil *state*, on $G_{max}$ are not taken into account correctly. Indeed, if the models had fully captured the effects of void ratio and confining pressure, no dependency of $\ln(G^m_{max}/G^p_{max})$ to the state parameter should have been observed. Similar dependencies and trends are also observed in the data for the decomposed granite as shown in Fig. 3. In this figure, for SR and WT expressions, different trends are observed which correspond to the tests conducted on specimens at different initial densities. Notice that in Figs. 2 and 3, only results for confining pressures less than 1 MPa are presented to avoid complications due to particle crushing, which can alter the slope of the critical state line [26,32,33]. As discussed by Russell and Khalili [32,33], the effect of particle crushing is negligible for quartz sands for confining pressures up to 1 MPa and the critical state line can be approximated with a straight line for all practical purposes. Finally, the results for SAP expression for decomposed granite are not presented in Fig. 3 as the expression is valid only for sands with coefficient of uniformity less than 9.7 ($C_u \leqslant 9.7$).

**Table 4**
Experimental program.

| Test soil | $e_o$ | |
|---|---|---|
| W1 | 0.75 | |
| W2 | 0.85 | |
| N1 | 0.75 | |
| N2 | 0.85 | |
| US1 | 0.75 | |
| US2 | 0.85 | |
| BL1-1 | 0.7 | Used in determination of variation of x, A and n with coefficient of uniformity ($C_u$). |
| BL1-2 | 0.75 | |
| BL1-3 | 0.8 | |
| BL1-4 | 0.85 | |
| BL2-1 | 0.7 | |
| BL2-2 | 0.75 | |
| BL2-3 | 0.8 | |
| BL2-4 | 0.85 | |
| BL3-1 | 0.7 | |
| BL3-2 | 0.75 | |
| BL3-3 | 0.8 | |
| BL3-4 | 0.85 | |
| BL4-1 | 0.7 | |
| BL4-2 | 0.75 | |
| BL4-3 | 0.8 | |
| BL4-4 | 0.85 | |
| 50UB-50UBL-1 | 0.75 | Used in determination of variation of A and n with regularity ($\rho$). |
| 50UB-50UBL-2 | 0.85 | |
| 70UB-30UBL-1 | 0.75 | |
| 70UB-30UBL-2 | 0.85 | |
| 30UB-70UBL-1 | 0.75 | |

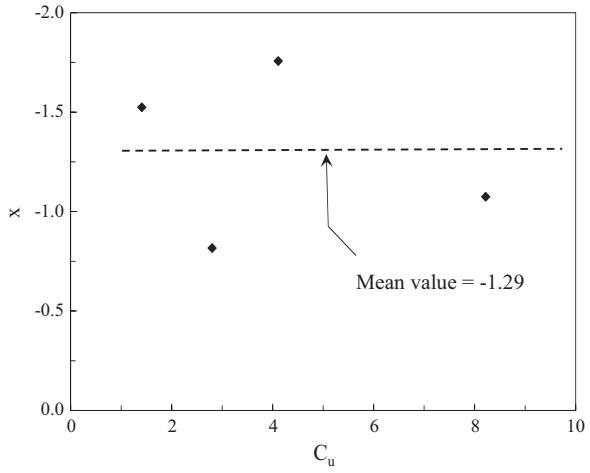


**Fig. 6.** Variation of void ratio power ($x$) with coefficient of uniformity ($C_u$) for Blue sands.

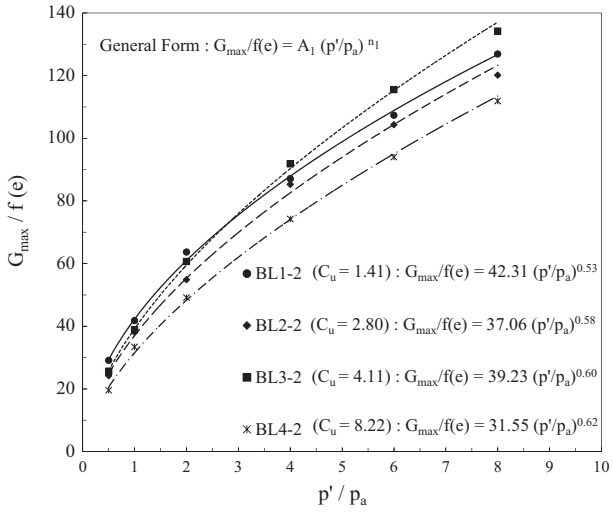


**Fig. 7.** Variation of normalized small-strain shear modulus ($G_{max}/f(e)$) with normalized confining pressure ($p'/p_a$) for Blue sands with different coefficients of uniformity at initial void ratio of 0.75.

## 4. Development of a new expression for $G_{max}$

The inability of the models of $G_{max}$ examined in capturing the *state* of the soil implies that the model parameters impacting the effects of $e$ and $p'$ have not been evaluated correctly and that they may be influenced by factors other than $C_u$ and $d_{50}$. For dry sand, apart from the grain size distribution, other influencing factors which may be considered include roughness and shape of the particles. At very small strains, the soil behavior is in the linear elastic range and hence all the small deformations are recoverable. From a micromechanical point of view, therefore there will be no slippage between the particles and consequently it may be concluded that the roughness of the sand grains may not have a considerable effect on $G_{max}$. On the other hand, as has been shown by a number of investigators, particle shape can have a significant influence on the small-strain shear modulus of sands [2,34,24,22].

To include the effect of particle shape, a new expression for $G_{max}$ is developed based on a comprehensive set of experimental data. First, adopting a power relationship for the void ratio function [16,18,22], we recall Eq. (1) in its most general form as:

$$G_{max} = A(C_u, d_{50}, shape) \times e^{x(C_u, d_{50}, shape)} \times \left(\frac{p'}{p_a}\right)^{n(C_u, d_{50}, shape)} \quad (2)$$

in which all model parameters $A$, $x$ and $n$ are rendered *a priori* functions of grain size distribution properties and particle shape. However, a careful examination of literature suggests that mean grain size ($d_{50}$) has little or no influence on parameters $A$ and $n$ [15,18,21,22], and $d_{50}$ and $C_u$ have little influence on $x$ as long as the particles are in the sand size range [15,18,22]. Similarly, there are no observed dependencies between $x$ and sand particle shape [22]. In addition, the effects of gradation and particle shape on parameters $A$ and $n$ are decoupled, yielding the following reduced form for $G_{max}$ expression:

$$G_{max} = A_1(C_u) \times A_2(shape) \times e^{x(C_u)} \times \left(\frac{p'}{p_a}\right)^{n_1(C_u) \times n_2(shape)} \quad (3)$$

in which the dependencies of the model parameters to coefficient of uniformity ($C_u$) and particle shape must be determined using a targeted program of laboratory testing.

## 5. Experimental work

Ten sands with different grain size distribution curves, covering a wide range of particle shapes, were selected to explore

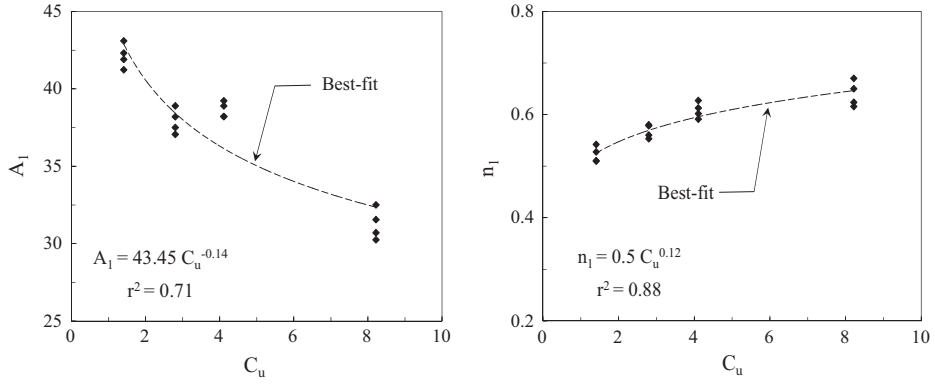


**Fig. 8.** Variation of parameters $A_1$ and $n_1$ with coefficient of uniformity ($C_u$).

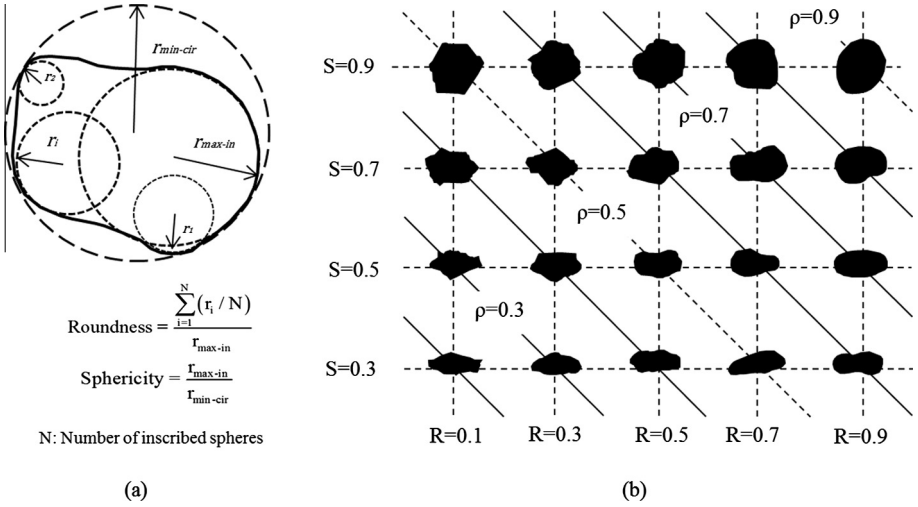


**Fig. 9.** Particle shape characterization chart (modified from Krumbein and Sloss [37]).

**Table 5**
Particle shape descriptors of the tested sands.

| Test sand | Particle shape descriptors[a] | | | | | |
|---|---|---|---|---|---|---|
| | R (MV) | S (MV) | $\rho$ (MV) | R (SD) | S (SD) | $\rho$ (SD) |
| W | 0.71 | 0.76 | 0.74 | 0.14 | 0.11 | 0.13 |
| N | 0.64 | 0.73 | 0.69 | 0.15 | 0.13 | 0.14 |
| US | 0.61 | 0.76 | 0.69 | 0.12 | 0.09 | 0.11 |
| BL1 | 0.24 | 0.51 | 0.38 | 0.12 | 0.18 | 0.15 |
| BL2 | 0.24 | 0.51 | 0.38 | 0.12 | 0.18 | 0.15 |
| BL3 | 0.24 | 0.51 | 0.38 | 0.12 | 0.18 | 0.15 |
| BL4 | 0.24 | 0.51 | 0.38 | 0.12 | 0.18 | 0.15 |
| 50UB-50UBL | 0.36 | 0.61 | 0.49 | 0.14 | 0.17 | 0.15 |
| 70UB-30UBL | 0.41 | 0.65 | 0.53 | 0.15 | 0.16 | 0.15 |
| 30UB-70UBL | 0.31 | 0.57 | 0.44 | 0.13 | 0.17 | 0.15 |

[a] R: Roundness, S: Sphericity, $\rho$: Regularity, MV: Mean value, SD: Standard deviation.

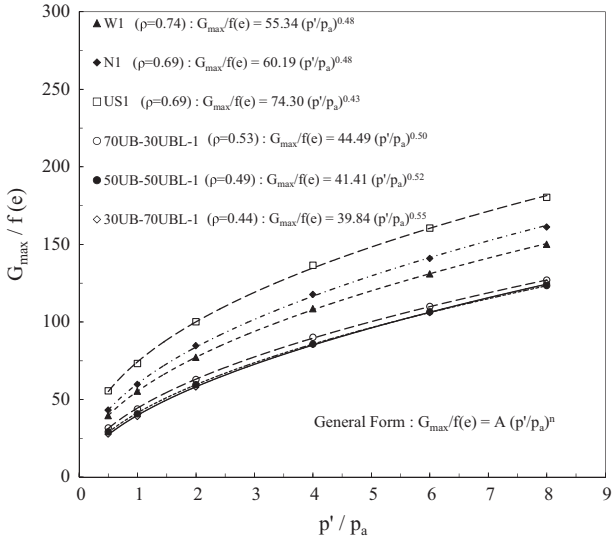


**Fig. 10.** Variation of normalized small-strain shear modulus with normalized confining pressure for different sand specimens with initial void ratio of 0.75 along with the best-fits according to Eq. (1).

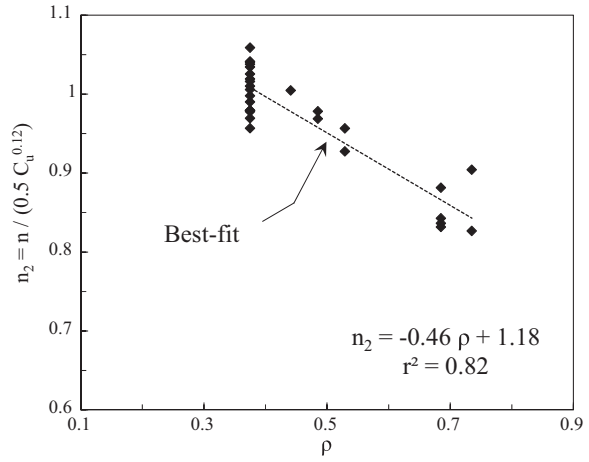


**Fig. 11.** Variation of $n_2$ parameter with regularity.

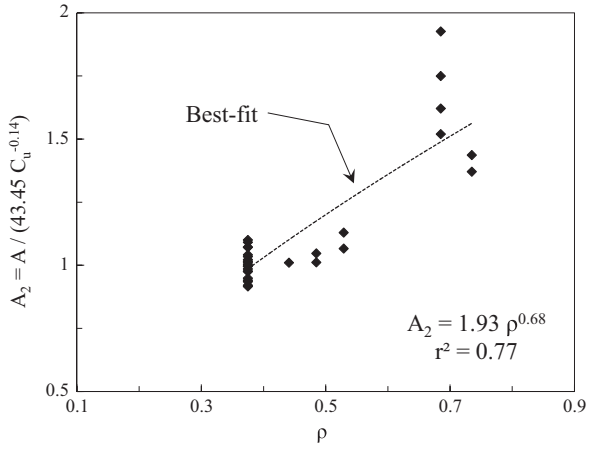


**Fig. 12.** Variation of $A_2$ parameter with regularity.

dependencies of $A_1$, $A_2$, $x$, $n_1$ and $n_2$ in Eq. (3) to $C_u$ and particle shape. The basic properties of the test soils are summarized in Table 3 and their grading curves are depicted in Fig. 4.

A modified Stokoe-type resonant column apparatus [35] with fixed-free configuration was used to determine the small-strain shear modulus of the sands [36]. The specimens, 50 mm in diameter and 100 mm in height, were prepared in several layers

**Table 6**
Different sand properties used for verification of new model.

| Test sand | Laboratory material | Grading | | Particle shape descriptors | | | | | | Critical state line parameters | |
|---|---|---|---|---|---|---|---|---|---|---|---|
| | | $d_{50}$ | $C_u$ | R (MV) | S (MV) | $\rho$ (MV) | R (SD) | S (SD) | $\rho$ (SD) | $\lambda$ | $\Gamma$ |
| S | Sydney sand | 0.31 | 1.95 | 0.61 | 0.76 | 0.69 | 0.12 | 0.09 | 0.11 | 0.05 | 1.15 |
| B | Bricky sand | 0.47 | 2.19 | 0.48 | 0.71 | 0.60 | 0.16 | 0.15 | 0.16 | 0.22 | 2.13 |
| CBL | Crushed blue sand | 0.69 | 2.00 | 0.24 | 0.51 | 0.38 | 0.12 | 0.18 | 0.15 | 0.24 | 1.87 |

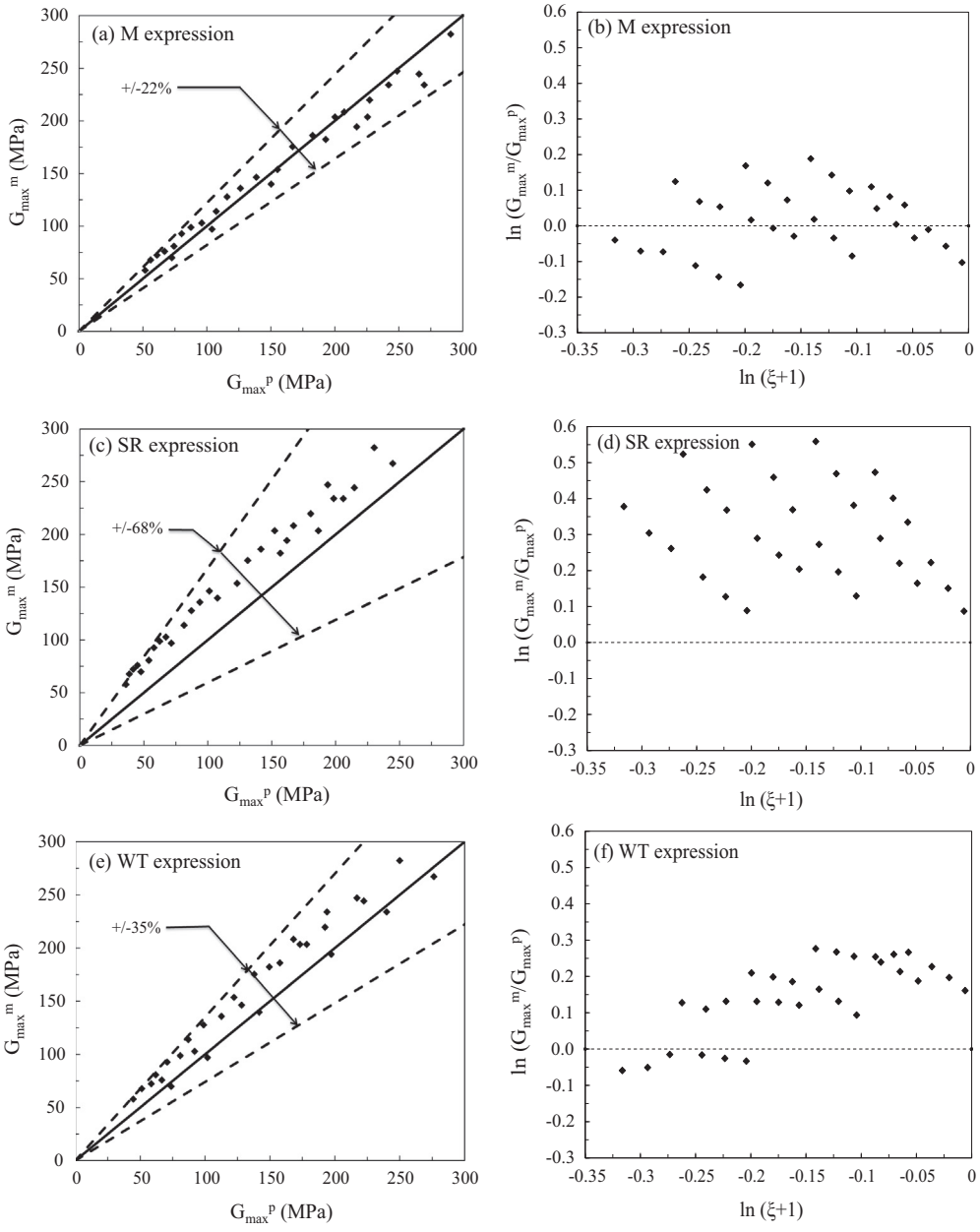


**Fig. 13.** Sydney sand: measured against predicted small-strain shear modulus and state parameter test results for different models.

to different initial void ratios by vibrating a known mass of soil to a predetermined height. Vibration was applied through a thin plastic rod with slightly rounded edges. By altering the vibration energy (i.e. duration) and thickness of the layers, samples were prepared at variable initial densities (see Table 4). All the resonant column tests were conducted in a dry state, in torsional mode and under isotropic condition.

In total, twenty-seven sets of tests were performed using different sands prepared at different void ratios, and at confining pressures of 50, 100, 200, 400, 600 and 800 kPa. Note that after the preparation of the sample and before application of the confining pressure, a vacuum of about 10 kPa was applied. While the sample was supported with vacuum, the dimensions of the sample were carefully measured to obtain the initial void ratio. Vacuum was

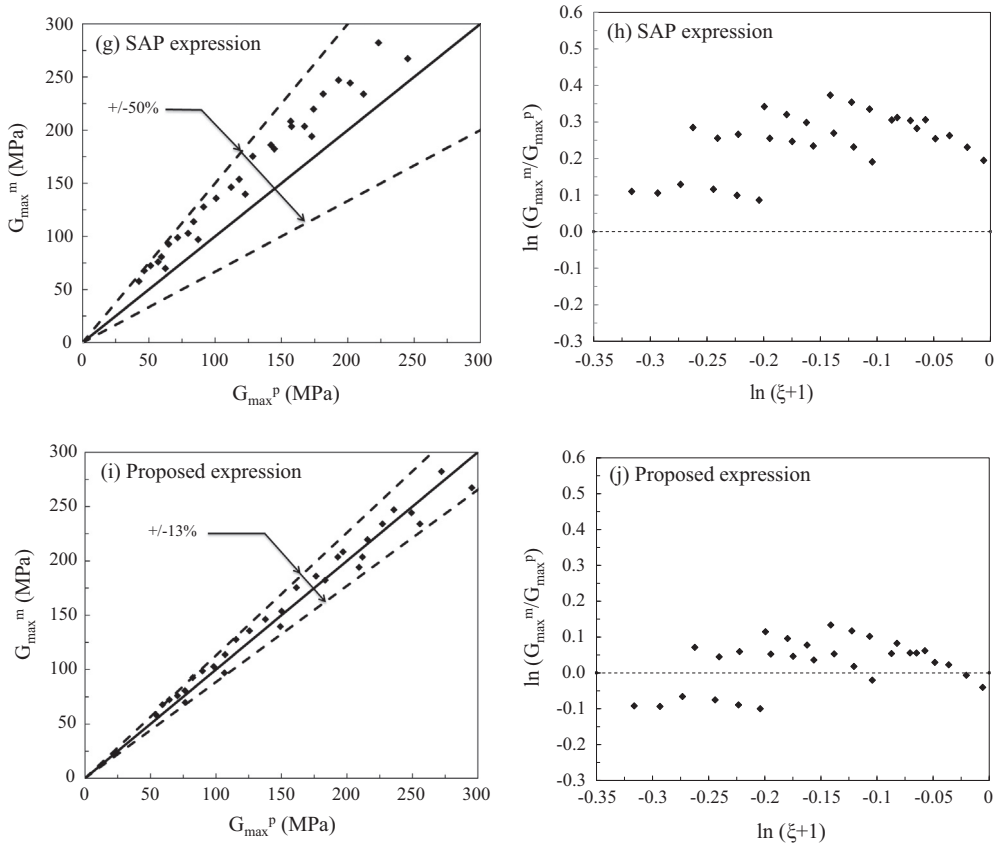


**Fig. 13** (*continued*)

then removed gradually during the application of the first isotropic confining pressure of 50 kPa. The analysis of the results was performed adopting the ASTM specification [36].

### 5.1. Variation of x with $C_u$

To establish dependency of the void ratio power, $x$, to coefficient of uniformity ($C_u$), the results from the resonant column tests performed on Blue sands (BL1–BL4), at different gradations and void ratios, but at constant particle shape and constant isotropic confining pressure (100 kPa), were examined (Fig. 5). Also included in Fig. 5 are the best-fits to constant $C_u$ data which is obtained by the least-square method. As can be observed, the values of $x$ obtained from the lines of best-fit in Fig. 5 show no discernible trend with the coefficient of uniformity, $C_u$, as depicted in Fig. 6. For the purposes of this study, a constant value of $x = -1.29$ is assumed leading to:

$$f(e) = e^{-1.29} \tag{4}$$

which is very similar to the relationship proposed by Jamiolkowski et al. [16]. This is also consistent with the work of Menq [18] and Senetakis et al. [22] who showed negligible and scattered dependency of $x$ on $C_u$. It is, however, inconsistent with the work of Wichtmann and Triantafyllidis [21] as is evident from Table 1.

### 5.2. Variation of $A_1$ and $n_1$ with $C_u$

To examine dependency of $A_1$ and $n_1$ on $C_u$, the tests carried out on Blue sands at a specific particle shape but different gradations ($C_u$ values) and initial void ratios, under a range of isotropic confining pressures (50–800 kPa) were considered. The variations of normalized small-strain shear modulus, $G_{max}/f(e)$, with normalized confining pressure, $p'/p_a$, for different sand gradations and for typical initial void ratio of 0.75 are shown in Fig. 7. Once again, the coefficients of best-fit to the data were used to establish the variations of $A_1$ and $n_1$ with the coefficient of uniformity (Fig. 8). As can be seen from this figure, $A_1$ has a descending, while $n_1$ has an ascending relationship with the coefficient of uniformity. Adopting a power best-fit trend, the following general expressions were obtained for the variation of $A_1$ and $n_1$:

$$A_1 = 43.45 \times C_u^{-0.14} \tag{5}$$

$$n_1 = 0.50 \times C_u^{0.12} \tag{6}$$

### 5.3. Particle shape effect on $A_2$ and $n_2$

To account the particle shape effect, one must first describe and assign a numerical value to the particle shape. This is achieved using the methodology originally proposed by Krumbein and Sloss [37] (Fig. 9). In this approach, the shape of a particle is characterized by two descriptors: (i) roundness (R) and (ii) sphericity (S). Roundness is expressed as the ratio of the average radius of curvature of the surface features to the radius of the largest sphere inscribed in the particle of the sand. Sphericity is defined as the ratio between the radius of the largest inscribed sphere in the particle to the radius of the smallest circumscribed sphere to the particle, as shown in Fig. 9a. Later, Cho et al. [24] introduced regularity ($\rho$) as the shape descriptor that incorporated the effects of both roundness and sphericity and quantified it as the arithmetic average value between sphericity and roundness. Cho et al. [24] showed that particle shape effects may be solely expressed through the variable $\rho$.

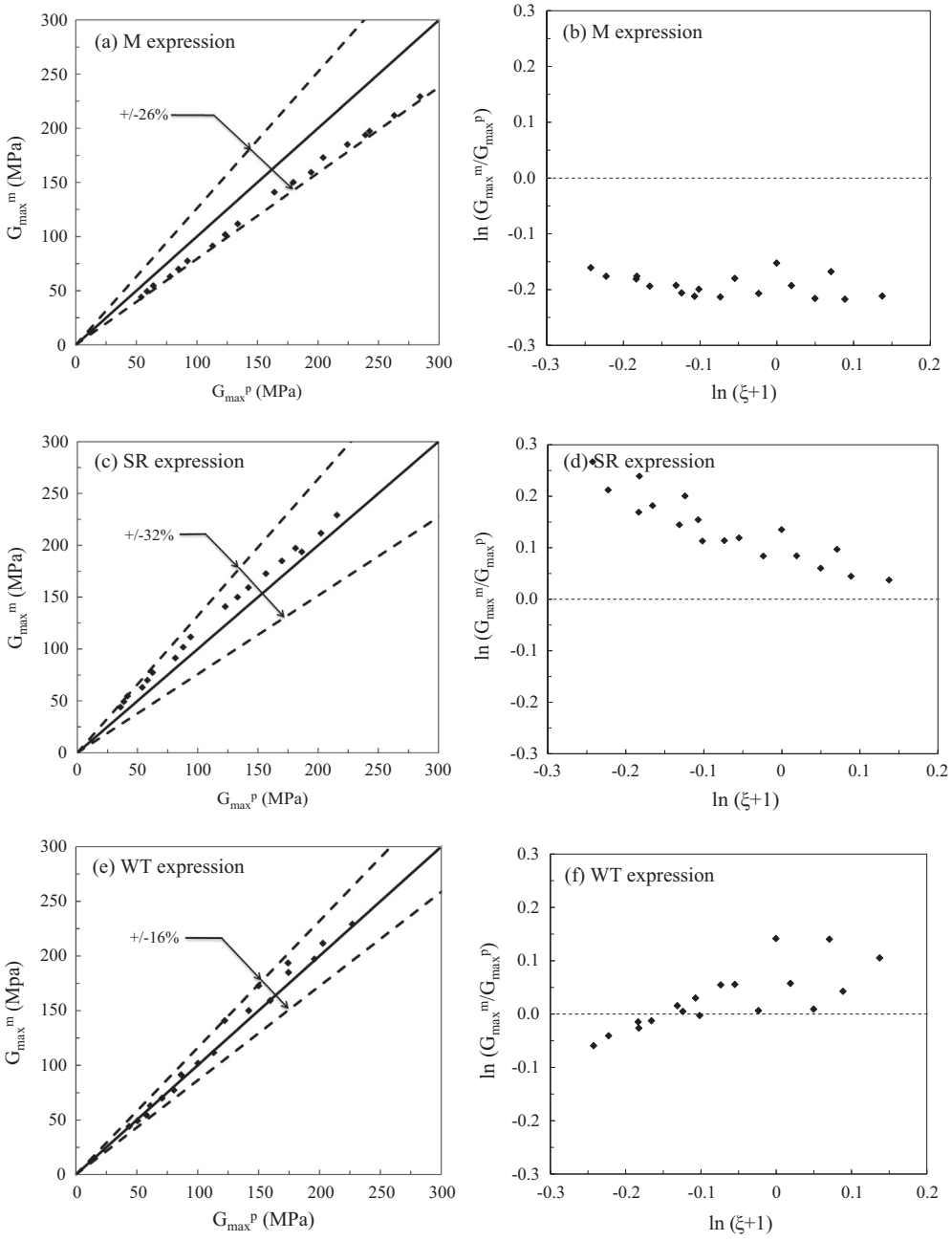


**Fig. 14.** Bricky sand: measured against predicted small-strain shear modulus and state parameter test results for different models.

The approach used in determining the regularity for each test soil included: (i) random selection of thirty particles from the parent material for observation under an optical microscope (ii) determination of a value for R (roundness) and a value for S (sphericity) for each particle based on the chart shown in Fig. 9b, and (iii) determination of the mean value (MV) of particle shape parameters along with the corresponding standard deviations (SD) for the thirty grains from each sand. Mean values and standard deviations of the shape descriptors for the test sands using this approach are summarized in Table 5. As can be noted from this table, the values of standard deviations for all sands and particle shape descriptors are almost in the same range, confirming the independency of SD values to the roundness, sphericity and regularity. All values of R and S were obtained independently from two operators for consistency.

To determine the dependency of $A_2$ and $n_2$ to the particle shape factor, $\rho$, the tests carried out on different sands with specific values of $C_u$ and $e$ but different particle shape parameter, $\rho$, under a range of isotropic confining pressures (50–800 kPa) were considered. Fig. 10 shows a typical set of results for the specimens with an initial void ratio of 0.75. Once again, the small-strain shear moduli are normalized against the void ratio function (Eq. (4)) and the normalized modulus is plotted against the normalized mean effective stress. Model parameters $A$ and $n$ were obtained from the best-fit power trend for soils with different regularity shape factor. A range of soils from fairly rounded (sample W1) to fairly angular (sample 30UB-70UBL-1) were used in the analysis.

Normalizing the values of $A$ and $n$ obtained from all data with respect to $A_1$ and $n_1$ expressions presented in Eqs. (5) and (6), the effect of particle shape, $\rho$, on $A_2$ and $n_2$ can be isolated as

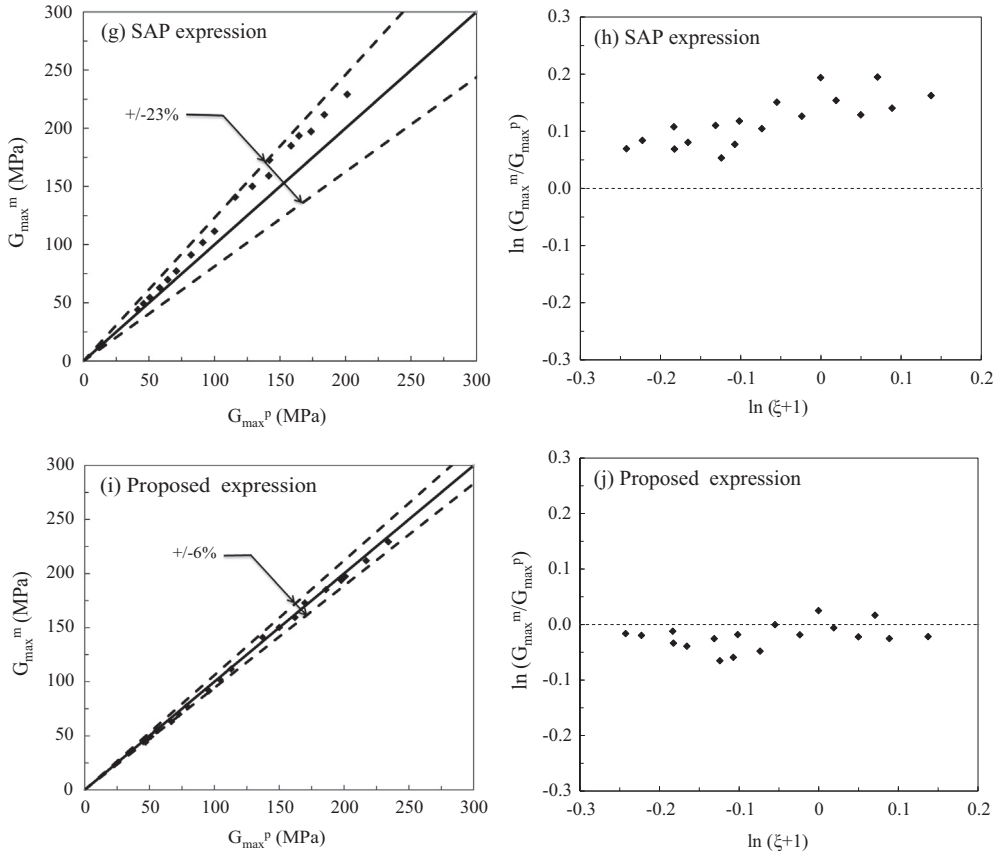


**Fig. 14** (*continued*)

depicted in Figs. 11 and 12. In both figures, strong trends are observed for the variation of $A_2$ and $n_2$ with particle shape, demonstrating the importance of inclusion of shape factor, $\rho$, in the $G_{max}$ expression.

### 5.4. Proposed model for small-strain shear modulus of sand

Using the best-fit Eqs. (5) and (6), and Figs. 11 and 12, derived for model parameters, it is now possible to present an expression for $G_{max}$ that takes into account the effect of grain size distribution, particle shape, void ratio and confining pressure:

$$G_{max} = \left(84C_u^{-0.14}\rho^{0.68}\right) \times e^{-1.29} \times \left(\frac{p'}{p_a}\right)^{(C_u^{0.12})(-0.23\rho+0.59)} \quad (7)$$

## 6. Verification

To verify the proposed model for small-strain shear modulus of sands and to compare the performance with some of the widely used models from the literature, the results of three independent series of resonant column tests on three different sands with a wide range of gradation and particle shape were considered. The first soil is Sydney sand, a poorly-graded quartz soil with sub-rounded to rounded particles, the second soil is Bricky sand, again a poorly-graded sand but with sub-angular particles, and the third is Crushed Blue sand with angular particles. Companion (three to four) consolidated drained (CD) triaxial tests were performed on each test soil to determine the critical state parameters. As mentioned previously, for the range of pressures used in this study (50–800 kPa), the effect of particle crushing was considered negligible and the CSL was approximated with a straight line [32,33]. Various properties of these sands are summarized in Table 6.

Sydney sand samples were tested at five different initial void ratios of 0.66, 0.70, 0.75, 0.80 and 0.85, while Bricky sand specimens were tested at three initial void ratios of 0.75, 0.80 and 0.85. The tests on Crushed Blue sand were carried out at initial void ratios of 0.70, 0.75, 0.80 and 0.85. Each sample was tested along an isotropic compression path at 50, 100, 200, 400, 600 and 800 kPa confining pressures.

The four previously presented expressions for $G_{max}$ from the literature (Table 1) in addition to the proposed expression (Eq. (7)) were used in the analysis. For all the expressions, the comparison between measured small-strain shear modulus ($G_{max}^{m}$) and predicted small-strain shear modulus data ($G_{max}^{p}$) as well as $\ln(G_{max}^{m}/G_{max}^{p})$ versus $\ln(1+\xi)$, were examined (Figs. 13–15). As can be observed, the proposed expression remarkably outperforms the other expressions from the literature. The maximum error involved in the M, SR, WT and SAP predictions (for the three soils) were 59%, 68%, 47% and 50%, respectively, while it was only 13% for the expression proposed. Of the expressions from the literature, M expression produces the best predictions for soils containing sub-rounded to rounded particles (Sydney sand), the WT expression is the most appropriate for sub-angular particles (Bricky sand), and SAP and SR expressions are the most appropriate for sands with sub-angular to angular particles (Crushed Blue sand). None of the expressions from the literature are valid for the range of particle shapes considered.

Figs. 13–15 demonstrate once again the usefulness of the state parameter in the evaluation of appropriateness of a $G_{max}$ model. If only graphs of measured versus predicted small-strain shear

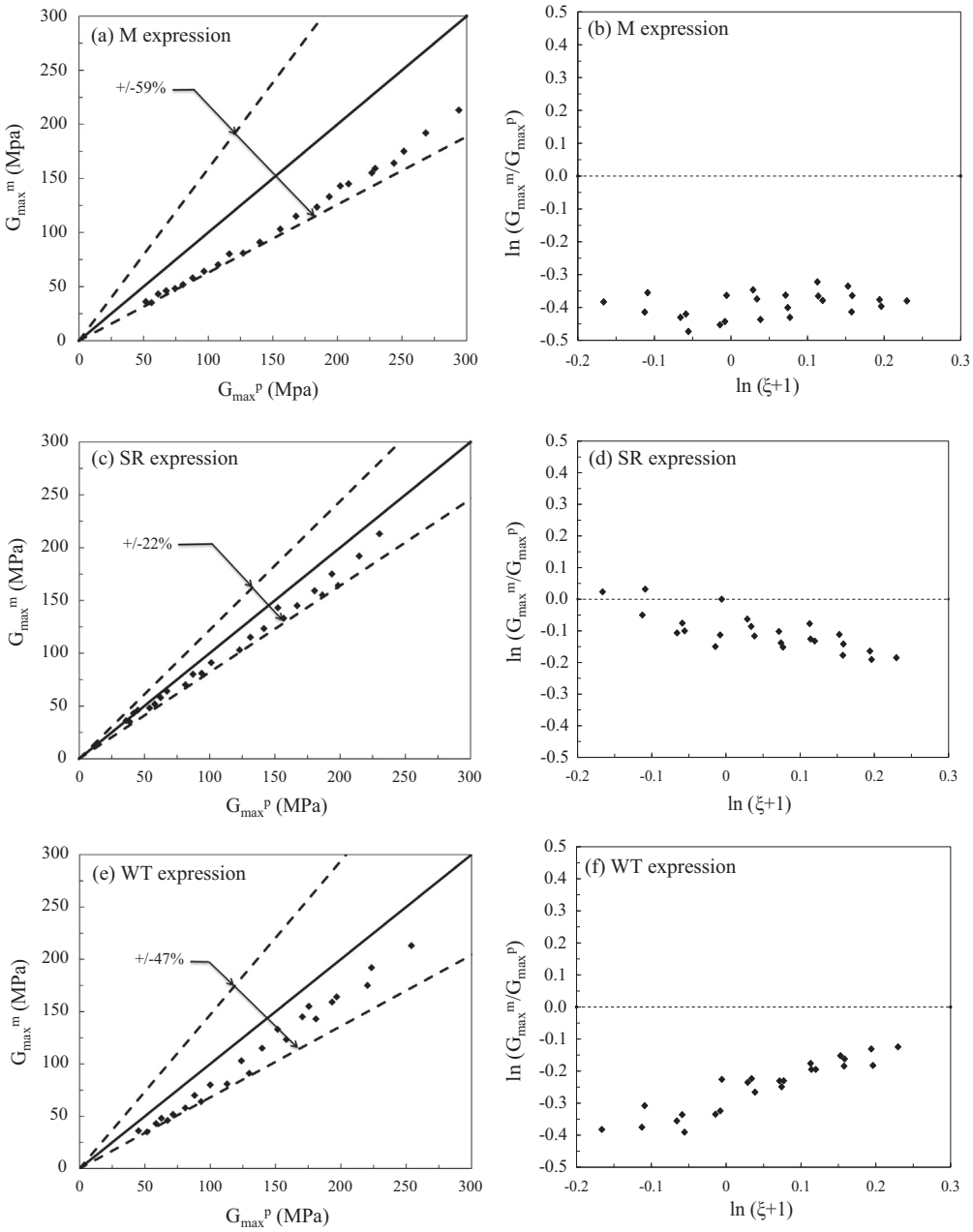


**Fig. 15.** Crushed Blue sand: measured against predicted small-strain shear modulus and state parameter test results for different models.

modulus values are adopted for comparison and verification of the models, it may be difficult to examine the appropriateness of the model as a general $G_{max}$ predictor. However when the results are presented against the state parameter, even for the soils for which the model is calibrated against, the fundamental flaws of the model in capturing the effects of void ratio and confining pressure, and hence its generality, are revealed.

## 7. Concluding remarks

A novel approach, based on the critical state soil mechanics framework, has been proposed to verify the accuracy of four previously proposed expressions for small-strain shear modulus of dry and saturated sands. It has been shown that none of the formulas examined could adequately capture the effects of void ratio and confining pressure on small-strain shear modulus. This deficiency has been attributed to overlooking the effect of sand particle shape on the model parameters associated with the void ratio and the confining pressure. A comprehensive experimental program has been performed using a resonant column apparatus to quantify the combined influences of the grain size distribution and particle shape on the small-strain shear modulus of sands. Using the regularity as a measure of particle shape, a new expression for small-strain shear modulus of sand has been proposed incorporating the effects of grain size distribution properties, particle shape, void ratio and confining pressure in a systematic and consistent manner. Three sets of experimental data on different sands have been used to demonstrate the validity of the proposed model. It is shown that each of the models examined from the literature is valid only for a specific range of particle shapes while the proposed

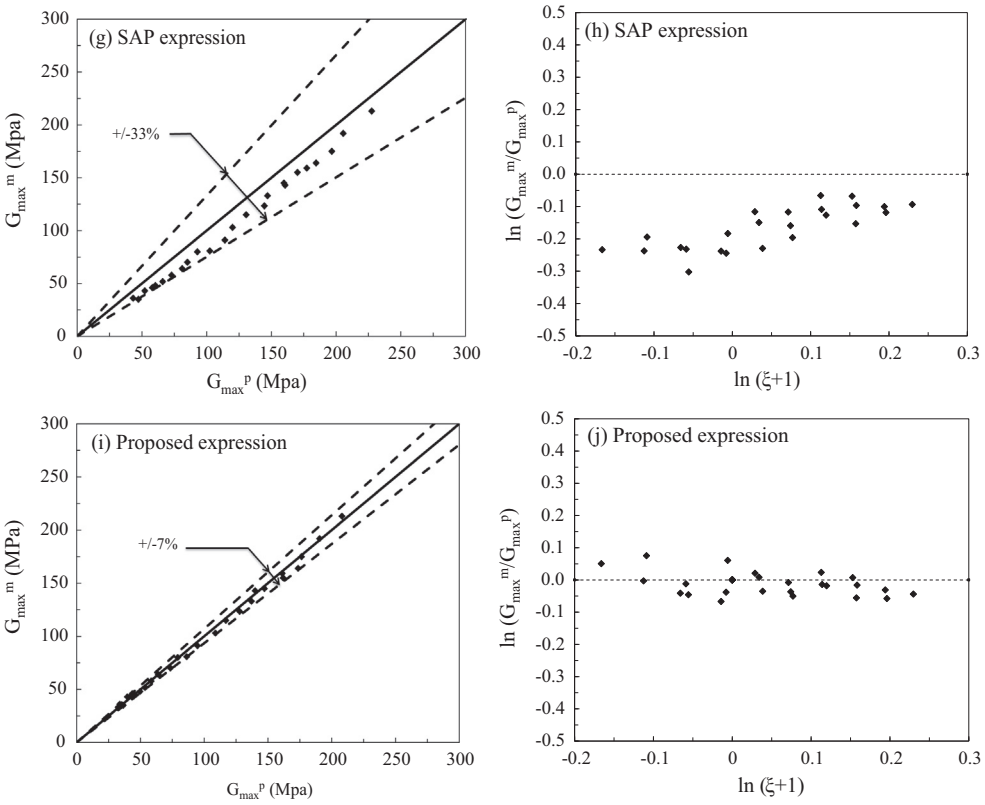


**Fig. 15** (*continued*)

model is general in nature, and can be equally applied to sands with different particle shapes.

## Acknowledgement

The anonymous reviewers are acknowledged for their constructive comments in improving the quality of the paper.

## References

[1] Reynolds JM. An introduction to applied and environmental geophysics. 2nd ed. New York: Wiley; 2011.
[2] Hardin B, Richart Jr FE. Elastic wave velocities in granular soils. J Soil Mech Found Div 1963;89(SM1):33–65.
[3] Hardin B. The nature of stress strain behaviour of soils. In: Proceedings of the geotechnical division speciality conference on earthquake engineering and soil dynamics. Pasadena, CA: ASCE; 1978. p. 3–90.
[4] Iwasaki T, Tatsuoka F, Takagi Y. Shear moduli of sands under cyclic torsional shear loading. Soils Found 1978;18(1):39–56.
[5] Viggiani G, Atkinson JH. Stiffness of fine-grained soil at very small strains. Geotechnique 1995;45(2):249–65.
[6] Hardin B. "Dynamic vs. static shear modulus for dry sand", Materials Research and Standards. Am Soc Test Mater 1965:232–5.
[7] Hardin B, Black W. Vibration modulus of normally consolidated clay. J Soil Mech Found, ASCE 1968;94(SM2):353–69.
[8] Hardin B, Black WL. Sand stiffness under various triaxial stresses. J Soil Mech Found Div 1969;92(SM2):27–42.
[9] Drnevich V, Hall J, Richart F. Effects of amplitude of vibration on the shear modulus of sand. In: Proceedings, international symposium on wave propagation and dynamic properties of earth materials. New Mexico; 1967. p. 189–99.
[10] Drnevich V, Richart F. Dynamic prestraining of dry sand. J Soil Mech Found, ASCE 1970;96(SM2):453–67.
[11] Hardin B, Drnevich V. Shear modulus and damping in soils: measurement and parameter effects. J Soil Mech Found Div 1972;18(6):603–24.
[12] Kokusho T. Cyclic triaxial test dynamic soil properties for wide strain range. Soils Found 1980;20(2):45–60.
[13] Chung RM, Yokel FY, Drnevich V. Evaluation of dynamic properties of sands by resonant column testing. Geotech Test J 1984;7(2):60–9.
[14] Yu P, Richart FE. Stress ratio effects on shear modulus of dry sands. J Geotech Eng 1984;110(3):331–45.
[15] Saxena SK, Reddy KR. Dynamic moduli and damping ratios for Monterey No. 0 sand by resonant column tests. Soils Found 1989;29(2):37–51.
[16] Jamiolkowski M, Leroueil S, Lo Priesti D. Design parameters from theory to practice. In: Proceedings of the international conference on geotechnical engineering for coastal development: geo-coast 1991. Yokohama, Japan: Coastal Development Institute of Technology; 1991. p. 877–917.
[17] Iwasaki T, Tatsuoka F. Effects of grain size and grading on dynamic shear moduli of sands. Soils Found 1977;17(3):19–35.
[18] Menq FY. Dynamic properties of sandy and gravelly soils. Ph.D. Dissertation. Austin (TX): University of Texas at Austin; 2003.
[19] Menq FY, Stokoe II KH. Linear dynamic properties of sandy and gravelly soils from large-scale resonant tests. In: Di Benedetto H, Doanh T, Geoffroy H, Sauzeat C, editors. Deformation characteristics of geomaterials. Lisse: Swets & Zeitlinger; 2003. p. 63–71.
[20] Hardin B, Kalinski ME. Estimating the shear modulus of gravelly soils. J Geotech Geoenviron Eng 2005;131(7):867–75.
[21] Wichtmann T, Triantafyllidis T. Influence of the grain-size distribution curve of quartz sand on the small strain shear modulus $G_{max}$. J Geotech Geoenviron Eng 2009;135(10):1404–18.
[22] Senetakis K, Anastasiadis A, Pitilakis K. Small strain shear modulus and damping ratio of quartz and volcanic sands. Geotech Test J 2012;35(6):964–80.
[23] Senetakis K, Madhusudhan BN. Dynamics of potentially fill-backfill material at very small strains. Soils Found 2015;55(5):1196–210.
[24] Cho GC, Dodds J, Santamarina JC. Particle shape effects on packing density, stiffness, and strength: natural and crushed sands. J Geotech Geoenviron Eng 2006;132(5):591–602.
[25] Been K, Jefferies MG. A state parameter for sands. Geotechnique 1985;35(2):99–112.
[26] Been K, Jefferies MG, Hachey J. The critical state of sands. Geotechnique 1991;41(3):365–81.
[27] Verdugo R, Ishihara K. The steady state of sandy soils. Soils Found 1996;36(2):81–91 [Tokyo, Japan].
[28] Wang, Y. Characterization of dilative shear failure in sand. MPhil thesis. Hong-Kong, China: Hong Kong University of Science and Technology; 1997.
[29] Riemer ME, Seed RB. "Factors affecting apparent positions of steady-state line". J Geotech Geoenviron Eng ASCE 1997;123(3):281–8.
[30] Li XS, Wang Y. Linear representation of steady-state line for sand. J Geotech Geoenviron Eng 1998;124(12):1215–7.
[31] Jovicic V, Coop MR. Stiffness of coarse-grained soils at small strains. Geotechnique 1997;47(3):545–61.
[32] Russell AR, Khalili N. Drained cavity expansion in sands exhibiting particle crushing. Int J Numer Anal Meth Geomech 2002;26:323–40.

[33] Russell AR, Khalili N. A bounding surface plasticity model for sands exhibiting particle crushing. Can Geotech J 2004;41:1179–92.
[34] Edil TB, Luh G-F. Dynamic modulus and damping relationships for sands. Soil Dyn Earthquake Eng 1978;1:394–409.
[35] Cascante G, Santamarina C, Yassir N. Flexural excitation in a standard torsional-resonant column. Can Geotech J 1998;35:478–90.
[36] ASTM. Standard test methods for modulus and damping of soils by the resonant column method. D4015-92. Annual book of ASTM standards. USA: ASTM International; 1992.
[37] Krumbein WC, Sloss LL. Stratigraphy and sedimentation. 2nd ed. San Francisco: Freeman and Company; 1963.